Cross talk between DevS sensor kinase homologue, Rv2027c, and DevR response regulator of *Mycobacterium tuberculosis*

Deepak Kumar Saini, Vandana Malhotra, Jaya Sivaswami Tyagi*

Department of Biotechnology, All India Institute of Medical Sciences, Ansari Nagar, New Delhi 110029, India

Received 24 December 2003; revised 13 February 2004; accepted 17 February 2004

First published online 8 April 2004

Edited by Gianni Cesareni

Abstract Rv2027c is a putative orphan histidine sensor kinase that bears strong homology to DevS of the hypoxia-responsive DevR–DevS two-component system in *M. tuberculosis*. The cytosolic C-terminal domain of Rv2027c protein ($Rv2027c_{194}$) was overexpressed in *E. coli* and biochemically characterized. $Rv2027c_{194}$ underwent autophosphorylation at a conserved His^{392} residue and engaged in phosphotransfer with DevR response regulator. The rates of autophosphorylation and the stabilities of the phosphorylated species were broadly similar in Rv2027c and DevS. However, unlike DevS, Rv2027c utilized Ca^{2+} as an alternative divalent ion during autophosphorylation. In contrast to DevS which completed phosphotransfer to DevR in 5–10 min, phosphotransfer from Rv2027c∼P was only partial at 30 min. Unlike *devS* transcription that was hypoxia-responsive, Rv2027c transcript levels were not upregulated from basal levels during hypoxia. The differential regulation of *devS* and *Rv2027c* genes, the ability of Rv2027c to utilize Ca^{2+} as a divalent cation in autophosphorylation at physiological concentrations and to engage in phosphotransfer with DevR suggests that the DevR regulon could be modulated by more than one environmental cue relayed through DevS and Rv2027c.

Keywords: Two-component system; DevS and Rv2027c sensor kinase; DevR response regulator; Cross talk; Calcium; *M. tuberculosis*

1. Introduction

Two-component systems of bacteria play a major role in their adaptation to the environment. In its most basic form, the two-component system consists of a histidine sensor kinase and a response regulator [1]. These systems use transient phosphorylation of the sensory and regulatory proteins at conserved residues for transducing extracellular or intracellular signals, thereby leading to an appropriate cellular response [2]. Such phosphorylation-based signalling has been established for five of eleven systems in *M. tuberculosis*, RegX3–SenX3 [3], TrcR–TrcS [4], MprA–MprB [5], PrrA–PrrB [6] and DevR–DevS (Rv3133c–Rv3132c/DosR–DosS) [7]. The genes encoding two-component systems are generally located adjacent to each other and are also coexpressed. The presence of seven 'orphan' genes coding for histidine kinases or response regulators but without the genes coding for the other component of proteins of two-component systems adjacent to them was an intriguing finding derived from determination of the genome sequence of *M. tuberculosis* H37Rv [8]. For instance, the gene encoding a potential sensor kinase, Rv2027c, is not adjacent to a gene encoding a response regulator. Since Rv2027c bears strong homology with DevS [8], there exists a possibility that diverse signals sensed by DevS and Rv2027c could generate a similar genetic response by signalling to a common response regulator protein, DevR. In this paper, we report for the first time the likely function of the orphan histidine kinase, Rv2027c. We have established Rv2027c to be a bonafide sensor kinase that undergoes autophosphorylation at a conserved histidine residue and communicates with DevR through a phosphotransfer reaction. Its unique metal ion requirement and physiological relevance are discussed.

2. Materials and methods

2.1. Bacterial strains, media, growth conditions and plasmids

Escherichia coli DH5α (Invitrogen Inc., USA) and XL1Blue (Stratagene Inc., USA) were used for routine cloning and *E. coli* BL23 (DE3) (gift from Dr. S. Vijaya, Indian Institute of Science, Bangalore) for protein production. Antibiotics, when required, were used at the following concentrations: ampicillin at 100 μg/ml, hygromycin at 200 μg/ml in *E. coli* and 25 μg/ml in *M. smegmatis*. *E. coli* was grown in LB media, while *M. tuberculosis* H37Rv (kindly provided by Dr. R.F. Silver, Case Western Reserve University, Cleveland, USA) and *M. smegmatis* LR222 (gift from Dr. J. Crawford, CDC, Atlanta, USA) were cultured in Dubos–Tween Albumin broth (DTA). All routine recombinant DNA work was performed as described [9]. The cytosolic domain-coding portion of $Rv2027c_{194}$ gene (amino acids 380–573) of *M. tuberculosis* H37Rv was amplified using gene-specific primers, 2027bamf (5′ GCGAGAAGTGGAGGATCCTGACC 3′) and 2027bamr (5′ GGATTGCGCGGATCCGTCGAC GCC 3′, engineered *Bam*HI restriction site is underlined), and inserted in pPROEx-HTc expression vector as described [7] to generate plasmid pDSH194. The reporter vector pFPVH was generated by inserting a hygromycin resistance cassette from pGEMT-Hyg (obtained as a gift from Dr. A. Ranganathan, ICGEB, New Delhi) in the green fluorescent protein (GFP) reporter vector, pFPV27 at the *Nsi*I site [10].

2.2. Overexpression of recombinant protein

$Rv2027c_{194}$ protein was overexpressed, purified and refolded using an established matrix-assisted protein renaturation protocol as described [11].

* Corresponding author. Fax: +91-11-2658-8663.
E-mail address: jstyagi@aiims.ac.in (J.S. Tyagi).

Abbreviations: cGMP, cyclic GMP; GAF, cyclic GMP (cGMP) – regulated cyclic nucleotide phosphodiesterases, adenyl cyclases and bacterial transcriptional regulator FhlA; GFP, green fluorescent protein; USP, Universal stress protein

0014-5793/$22.00 © 2004 Federation of European Biochemical Societies. Published by Elsevier B.V. All rights reserved.
doi:10.1016/j.febslet.2004.02.092

2.3. Site-directed mutagenesis

H392Q point mutation was introduced into pDSH194 using the QuikChange™ site-directed mutagenesis kit (Stratagene Inc., USA) and the mutagenic oligonucleotides H392Qf (5′ GCACGTGATCTGCAAGACCACGTCATCCAG 3′) and H392Qr (5′ CTGGATGACGTGGTCTTGCAGATCACGTGC 3′). The mutagenesis was verified by automated DNA sequencing using 377 ABI Prism DNA sequencer.

2.4. In vitro phosphorylation assays

Rv2027c$_{194}$ (15 μM) was autophosphorylated by incubating it with 5 μCi of γ[^{32}P] ATP (5000 Ci/mmol, BRIT, India) in 10 μl reaction buffer (50 mM Tris·Cl, pH 8.0, 50 mM KCl, 25 mM $MgCl_2$, and 50 μM ATP) at 25°C for 0–24 h. Standard reactions were performed as above for 60 min. For stability analysis, radiolabelled Rv2027c$_{194}$∼P was prepared in a 60 min reaction and incubated for up to 20 h after removal of unincorporated ATP and $MgCl_2$ by filtration of the reaction mixture through a 10 kDa Nanosep device. To study phosphotransfer, Rv2027c$_{194}$ (15 μM) was autophosphorylated for 60 min, then DevR (20 μM) was added to the reaction mixture and incubated at 25 °C for the indicated time periods. In all phosphorylation assays, samples were analyzed by SDS–PAGE and the gels were autoradiographed.

2.5. RT-PCR

Mycobacterium tuberculosis H37Rv was grown in DTA broth (100 ml in a 500 ml Erlenmeyer flask) as aerobic culture to late logarithmic phase with shaking at 37 °C (OD_{600} ∼0.7–0.8), after which 13 ml culture aliquots were aseptically transferred to 15 ml polystyrene conical tubes (Corning Inc., USA), sealed and kept without stirring for 48 h (hypoxic cultures). Methylene blue fading occurred in control tubes at 48 h indicating the setting in of hypoxia. RNA was isolated from these aerobic and hypoxic cultures and used for RT-PCR analysis as described [7]. The expression of *Rv2027c*, *hspX* and *devS* was analyzed using gene-specific primers after normalizing for 23S rRNA transcripts. The following primers were used: *Rv2027c*, 2027f (5′ CACCCTGACAGGGCGAACGTT 3′) and Rv2027r (5′ GGTCGTAACCGCGCACCCCG 3′); *hspX*, hspXf (5′ CGCCACCCGCGGTCCCTCTT 3′) and hspXr (5′ GCTCGGTGCGCTCGGCCTTG 3′) and *devS*, devS1 (5′ ACTACGCC TGCACGAGCTGCT 3′) and N3 (5′ GTCCAGCCGTAACGGTTTGGG 3′). At least two lots of RNA were analyzed twice each by RT-PCR.

2.6. GFP assays

The *Rv2027c* and *hspX* promoter regions were amplified using appropriate primers as below: *Rv2027c*, 2027Pf (5′ TCAATCGGTACACATGGTGGTGCTCA 3′) and 2027Pr (5′ TGCGCTCAACCAACTGGTCTGGCTA 3′); *hspX*, hspXPf (5′ TCTGAAC GGCGGTTGGCAGACA 3′) and hspXPr (5′ CGGGAAGGGTGGTGGCCATTTG 3′). The amplified promoter fragments were inserted in the promoterless GFP reporter vector, pFPVH, at the *Eco*RV site. *M. smegmatis* cultures carrying the recombinant GFP constructs were grown in DTA containing hygromycin till early log phase, subcultured (using a starting OD_{600} of 0.05) and grown under aerobic conditions and hypoxic conditions as described above. At 48 h, ∼10^5 cells from both aerated (OD_{590} 1.2–1.5) and hypoxic cultures (OD_{590} 0.12–0.16) were analyzed for fluorescence in a multiwell spectrofluorimeter (Molecular Devices Inc., USA) using an excitation wavelength of 483 nm and an emission wavelength of 515 nm.

3. Results

3.1. Computational analysis of Rv2027c

Mycobacterium tuberculosis H37Rv genome analysis revealed the existence of a putative sensor histidine kinase of 573 amino acids, Rv2027c, without its accompanying response regulator that displayed 62.5% identity with DevS sensor kinase [12] over its entire length. Two GAF domains (present in cyclic GMP (cGMP) – regulated cyclic nucleotide phosphodiesterases, adenyl cyclases and bacterial transcriptional regulator FhlA and formerly thought to bind only cyclic GMP and now found to bind cyclic AMP as well [13]) mapped in the N-terminal domain of Rv2027c protein at a similar location as in DevS (Fig. 1A). These domains are ubiquitous modules present in a large number of signalling and sensory proteins and are reported to bind small molecule ligands such as cGMP and modulate their activity [13]. The presence of similarly located and organized GAF domains in Rv2027c and DevS proteins suggests that both the proteins are involved in processing similar/related signals and/or may be involved in the execution of similar outputs. The presence of only one transmembrane region (TM1) in the Rv2027c protein was deduced by TMpred analysis (online transmembrane domain-predicting software available at http://us.expasy.org). The C-terminal region sequences that comprise the catalytically active kinase core were also highly conserved in Rv2027c and DevS, particularly the amino acid sequences of the H box (containing the phosphorylatable histidine residue) and the N, D/G1 and G2 boxes involved in ATP binding [1]. BLAST analysis of the available mycobacterial genome databases indicated Rv2027c to be absent from all mycobacteria except *M. tuberculosis* and *M. bovis* (Table 1). The presence of *Rv2027c* orthologue in *M. bovis* BCG (Pasteur strain ATCC 35734) was established by PCR using *M. tuberculosis* gene-specific primers (not shown). The possession of an additional DevS-like sensor kinase in *M. tuberculosis* complex but not in other mycobacteria sequenced so far is striking and may be indicative of a unique role for it in these pathogens.

3.2. Genetic organization of Rv2027c

The genomic context of *Rv2027c* gene was very similar to that of DevS except that a *devR* homologue was absent. This suggested that this locus could have arisen through a partial gene duplication event from the *Rv3134c–devR–devS* locus accompanied by the loss of *devR*, hence its 'orphan' status (Fig. 1B). *Rv2027c* is flanked on either side by *Rv2026c* and *Rv2028c*, both of which are homologous to *Rv3134c* and display 30% and 40% identity, respectively, with the latter. All three genes code for proteins containing the Universal stress protein (USP) domain first identified in the Usp protein that is induced under a variety of stress conditions and is proposed to play a protective role in *E. coli* [14]. Proteins of this family are induced during stress responses in several other bacteria as well including mycobacteria [15]. There are numerous examples of gene redundancy such as this in *M. tuberculosis* [8] and could reflect a strategy used by the tubercle bacillus to keep 'back-up' copies of genes functioning in critical bacterial pathways. A second similarity between the two loci is their hypoxia-responsive character; the *devR–devS* genes map in a 12-gene hypoxia-responsive cluster [16], Bagchi, G. unpublished observations, while *Rv2027c* maps near a 5-gene hypoxia-responsive cluster that includes *hspX* (*acr*) but was itself not induced in hypoxia in *M. tuberculosis* [16].

A *devS* (*dosS*) knockout strain of *M. bovis* BCG was reported to be only moderately affected in hypoxic survival compared to a *devR* (*dosR*) mutant that showed a severe defect in hypoxic viability [17]. Similarly, a *devR* but not a *devS* mutant of *M. tuberculosis* was abrogated in the hypoxic expression of Acr [16]. Based on the significant similarity between DevS and Rv2027c and the phenotype of *devS* mutants, it was speculated that Rv2027c could participate in phosphosignalling [12,16]. Therefore, the possibility of Rv2027c to function as a sensor kinase and communicate with DevR was investigated in this study.

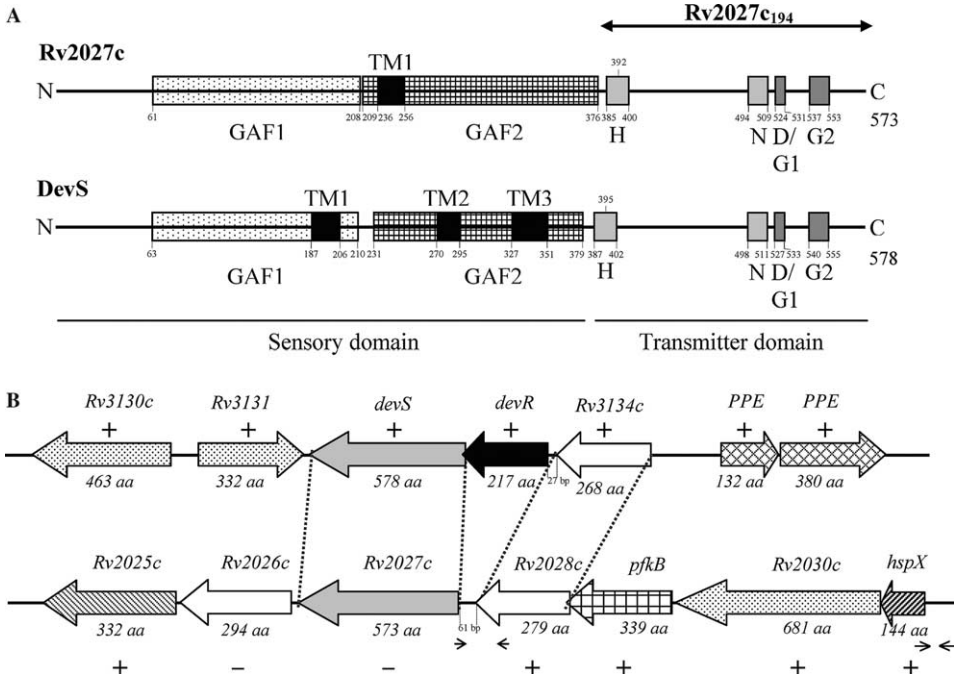

Fig. 1. (A) Organization of domains and boxes in Rv2027c and DevS proteins. Patterned boxes denote putative GAF domains; solid black boxes indicate the putative transmembrane (TM) regions; grey boxes represent H, N, D/G1 and G2 boxes (designated according to [1]). (B) Genetic organization of the *Rv2027c* and the *devR–devS* loci in *M. tuberculosis*. Genes of similar predicted function are represented by similar patterns. Plus and minus signs above/below individual genes indicate hypoxia response according to [16], and Bagchi, G. unpublished observations. Thin arrows denote primers used to amplify the putative *Rv2027c* and *hspX* promoter regions.

3.3. Purification of Rv2027c sensor kinase

The cytosolic catalytic domain of Rv2027c ($Rv2027c_{194}$, Fig. 1) was overexpressed in *E. coli*. The N-terminally His_6-tagged $Rv2027c_{194}$ protein, that essentially localized in inclusion bodies, was denatured and refolded to give a protein of 85–90% purity as judged by SDS–PAGE (Fig. 2).

3.4. Autophosphorylation of $Rv2027c_{194}$

During autophosphorylation of $Rv2027c_{194}$, maximum incorporation of labelled phosphate occurred at ~4 h, and ~100% of the label was retained by the protein between 4 and 24 h (Fig. 3A). $Rv2027c_{194}$ was not labelled in the presence of $\alpha[^{32}P]$ATP, indicating that phosphorylation occurred only through a γ-phosphate transfer from ATP and was not due to non-specific binding of ATP to the protein (data not shown).

Table 1
Orthologues of DevS and Rv2027c proteins in various finished and unfinished mycobacterial genomes

Mycobacterial species	Percent identity[a]	
	DevS	Rv2027c
M. tuberculosis H37Rv[b]	100	100
M. tuberculosis CDC1551[b]	100	100
M. tuberculosis 210[c]	89	99.5
M. bovis AF2122/97[b]	99	99
M. marinum[c]	79	–
M. smegmatis mc^2 155[c]	65	–
M. avium 104[c]	42	–
M. avium sub. *paratuberculosis* K-10[c]	42	–
M. leprae[b]	–	–

[a] Homology (%) is over the entire length of *M. tuberculosis* protein and the query protein in pairwise alignment.
[b] Annotated genome sequence.
[c] Genome sequence unfinished and unannotated.

When $Rv2027c_{194}$~P was purified away from ATP and incubated further, no decrease in signal was recorded till 20 h (Fig. 3B). These experiments suggest $Rv2027c_{194}$~P to be a stable species under the conditions tested with a half-life of >20 h. The stability of $Rv2027c_{194}$~P contrasted to that of sensor kinases such as NarX of *E. coli* and RegS of *Bradyrhizobium japonicum*, the half lives of whose phosphorylated forms were reported to range from 15 min to >1 h [18,19], but was similar to that of DevS, which demonstrated equivalent stability under similar conditions [7].

3.5. Confirmation of His^{392} residue as the site of phosphorylation in Rv2027c

The putative site of phosphorylation in Rv2027c, His^{392}, was mutated to Gln and analyzed in the phosphorylation reaction. $Rv2027c_{194}$-H392Q mutant protein was defective in autophosphorylation confirming His^{392} to be the target residue in the phosphorylation and establishing Rv2027c protein to be an authentic histidine sensor kinase (Fig. 3C).

3.6. Divalent ion utilization in Rv2027c autophosphorylation

The ability of $Rv2027c_{194}$ to utilize divalent cations during autophosphorylation was assessed. As with DevS, phosphorylation was optimal in the presence of Mg^{2+} (Fig. 4A, lane 1) and showed 50% efficiency in the presence of Ca^{2+} (Fig. 4A, lane 3). Mn^{2+} and Co^{2+} were also utilized at 50% and 40% efficiencies, respectively, based on quantitation of radioactivity incorporated in $Rv2027c_{194}$~P (Fig. 4A). The ability of $Rv2027c_{194}$ to be phosphorylated in the presence of Ca^{2+} emerged as a major difference between the activities of DevS and Rv2027c sensor kinases as DevS failed to utilize Ca^{2+} [7].

The effect of Ca^{2+} on autophosphorylation of $Rv2027c_{194}$ was examined further. A biphasic effect was noted in a

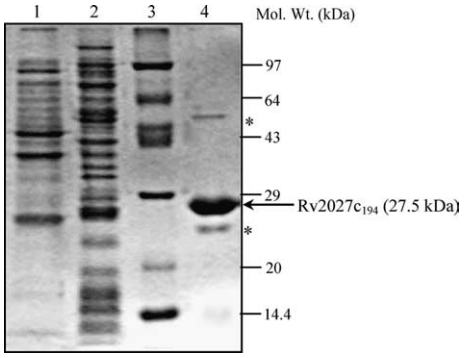

Fig. 2. SDS–PAGE (12.5%) profile of His_6-$Rv2027c_{194}$ purification. Lane 1, lysate of uninduced *E. coli* cells carrying expression construct pDSH194; lane 2, lysate of IPTG-induced cells carrying pDSH194; lane 3, protein molecular weight marker and lane 4, purified and refolded $Rv2027c_{194}$ protein. ∗, contaminating proteins.

concentration range of 10 nM to 100 mM; maximum and minimum phosphorylation occurred in the presence of 50 mM $CaCl_2$ and 1–5 mM $CaCl_2$, respectively. We have no explanation for the biphasic peaks of activity in the Ca^{2+} gradient, particularly since concentrations in excess of 5–10 mM are non-physiological. The activity peak at higher concentrations could be the result of in vitro perturbations. The net phosphorylation of $Rv2027c_{194}$ increased in a concentration-dependent manner on further reduction in Ca^{2+} concentration till 10 nM when an incorporation of ~60% of maximum was obtained (Fig. 4B and D). Like Ca^{2+}, Mg^{2+} was also utilized over a wide concentration range (mM to nM) except that peak phosphorylation was noted in the presence of 1 mM $MgCl_2$ and incorporation decreased at lower and higher concentrations (Fig. 4C). Ca^{2+} was a much better activator of Rv2027c in comparison to Mg^{2+} at low cation concentrations (Fig. 4D). Further, autophosphorylation of Rv2027c occurred efficiently in the presence of extremely low (nanomolar) concentrations of either Mg^{2+} or Ca^{2+} ions unlike DevS which was completely unresponsive to Ca^{2+} and needed at least 1–10 mM $MgCl_2$ to undergo phosphorylation (Fig. 4D). This differential effect of Ca^{2+} and Mg^{2+} on autophosphorylation of Rv2027c could reflect its ability to participate in phosphosignalling over a wide range of metal ion concentrations as occurs in extracellular vs. intracellular environments.

3.7. Phosphorylation of DevR by $Rv2027c_{194}$~P

DevR was rapidly phosphorylated by $Rv2027c_{194}$~P; peak incorporation into DevR was achieved within 2 min of initiating the reaction (Fig. 5A). However, phosphotransfer from $Rv2027c_{194}$ to DevR was not as efficient as that from $DevS_{201}$; a significant amount of phosphorylation remained associated with $Rv2027c_{194}$ at the end of 30 min (Fig. 5A) in contrast to DevS from which phosphosignal disappeared rapidly within 10–15 min [7]. $Rv2027c_{194}$~P was a stable species in the absence but not in the presence of DevR to which it transferred its phosphoryl group generating DevR~P. When $Rv2027c_{194}$~P was incubated with DevR-D54V, a phosphorylation-defective mutant derivative of DevR [7], dephosphorylation of Rv2027c~P was completely abrogated (Fig. 5B). This suggests that DevR decreases the stability of Rv2027c~P not by inducing an autophosphatase activity of Rv2027c, rather it is the transfer of the phosphoryl moiety from Rv2027c to DevR (that occurs very rapidly) which causes dephosphorylation of Rv2027c~P. No ion including Ca^{2+} could replace Mg^{2+} during phosphotransfer (Fig. 5C). Our finding was consistent with published reports that Mg^{2+} is utilized in the vast majority of phosphotransfer reactions that are catalyzed by the response regulator [2].

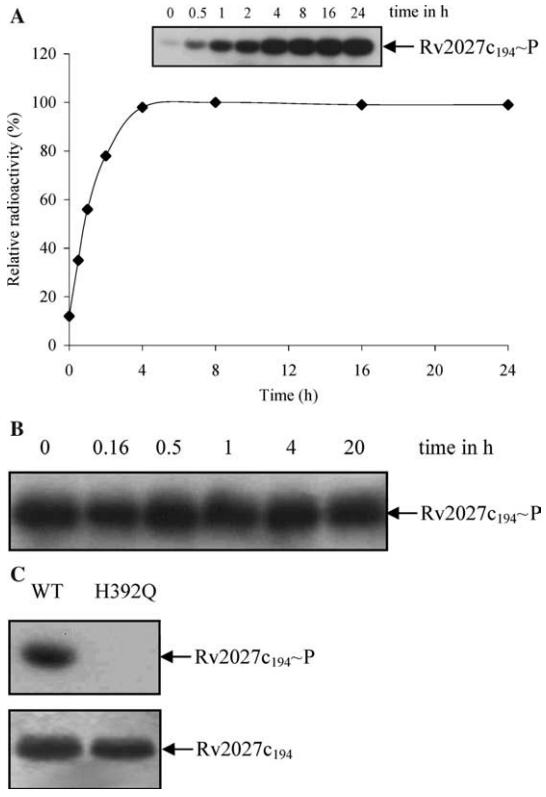

Fig. 3. (A) Time-dependent autophosphorylation of $Rv2027c_{194}$. $Rv2027c_{194}$ (15 μM) was incubated in reaction buffer as described. Samples were removed at indicated time points, chilled on ice with stop buffer and analyzed by SDS–PAGE. Gel slices corresponding to the labelled proteins were excised and the radioactivity incorporated was quantitated by liquid-scintillation counting. (B) Stability of radioactive $Rv2027c_{194}$~P. Radioactive $Rv2027c_{194}$~P was prepared as described and its stability was analyzed by incubation at 25 °C. (C) Phosphorylation of $Rv2027c_{194}$H392Q mutant protein. Wild type and mutant $Rv2027c_{194}$ proteins (15 μM each) were essentially phosphorylated as described earlier. The lower panel shows the Coomassie Brilliant Blue-stained gel profile of the top panel.

3.8. Rv2027c expression analysis

Rv2027c-specific transcripts were detected in aerobic cultures of *M. tuberculosis* confirming this gene to be active in terms of being expressed at the RNA level and having the potential to be translated into protein in vivo (Fig. 6, lane 1). Since *Rv2027c* is located in the vicinity of a hypoxia-responsive gene cluster containing *hspX* (*acr*), its expression in 48 h hypoxia-adapted cultures was also assessed and found unaltered although *devS* and *acr* transcripts were upregulated under those conditions by ~6.4-fold and ~1.6-fold, respectively (Fig. 6, lane 2). This observation was consistent with an earlier report wherein no change in *Rv2027c* expression was observed during hypoxia [16]. A possible explanation for the lack in hypoxic induction of *Rv2027c* is that it is independently transcribed from an upstream promoter (Fig. 1B). The small upstream intergenic region was accordingly analyzed for promoter activity using GFP as reporter, but it failed to show

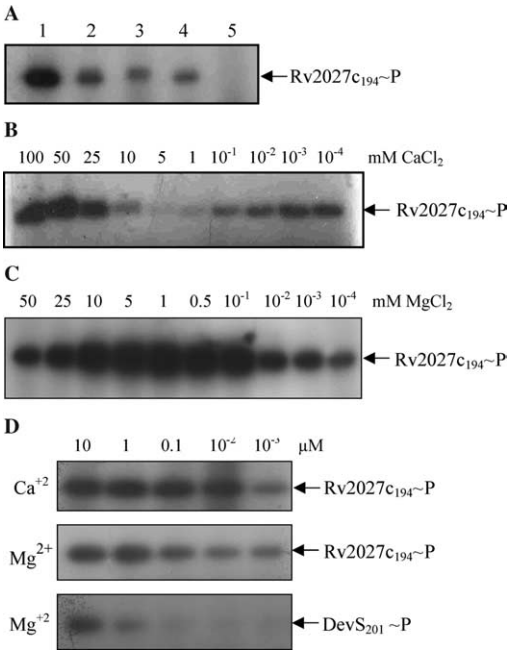

Fig. 4. (A) Divalent cation requirement in $Rv2027c_{194}$ autophosphorylation. $Rv2027c_{194}$ (15 μM) was autophosphorylated with $\gamma[^{32}P]$ ATP in reaction buffer containing divalent cations as mentioned. Lane 1, $MgCl_2$; lane 2, $MnCl_2$; lane 3, $CaCl_2$; lane 4, $CoCl_2$; lane 5, EDTA, 25 mM each. (B) Autophosphorylation of $Rv2027c_{194}$ in the presence of 100 nM–100 mM $CaCl_2$. (C) Autophosphorylation of $Rv2027c_{194}$ in the presence of 100 nM–50 mM $MgCl_2$. (D) Autophosphorylation of Rv2027c and DevS proteins (15 μM) in the presence of 1 nM–10 μM divalent ions in the reaction mixture. All studies to assess divalent cation utilization were performed in standard reactions as described in Section 2.4.

promoter activity under either aerobic or hypoxic conditions while the *acr* promoter was hypoxia-responsive (~4.5-fold) under identical conditions (data not shown). These results suggest that the *Rv2027c* promoter maps elsewhere within an upstream gene (*Rv2028c* or *pfkB*) or alternatively, that the promoter is not recognized in *M. smegmatis*. However, the latter possibility seems unlikely as the same putative promoter region failed to support GFP synthesis from a reporter plasmid in *M. bovis* BCG [20]. Another explanation for the lack of GFP expression using the *Rv2027c* putative promoter region could be the relatively low sensitivity of the GFP system if the *Rv2027c* promoter is not very strong.

4. Discussion

We have recently established *devR–devS* to encode a bonafide two-component system of *M. tuberculosis* [7]. In this study, we show Rv2027c to be a functional sensor kinase that engages in phosphotransfer with DevR protein. Further, we show that Rv2027c is expressed at equivalent levels under aerobic and hypoxic conditions in *M. tuberculosis* cultures.

In spite of the high degree of sequence and domain similarity between the two proteins, distinct differences were noted between DevS and Rv2027c in their autophosphorylation and phosphotransfer properties. Firstly, although the phosphorylated forms of DevS and Rv2027c are both stable, they are distinct with respect to the utilization of Ca^{2+} and Mg^{2+} during autophosphorylation. Secondly, *devS* and *Rv2027c*

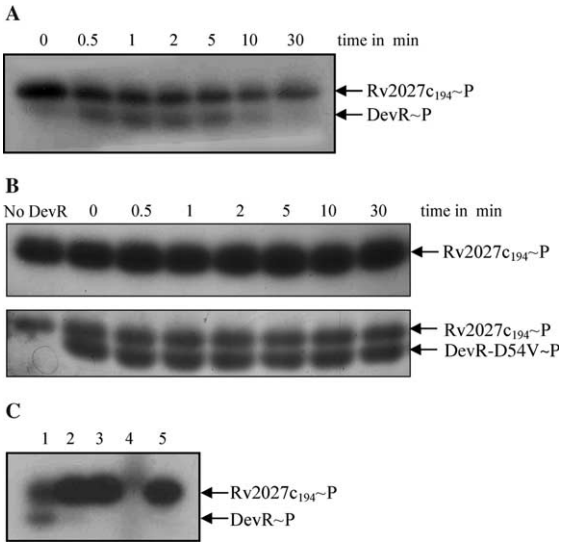

Fig. 5. (A) Phosphotransfer from $Rv2027c_{194}$~P to DevR. $Rv2027c_{194}$~P was prepared as described. DevR was added to $Rv2027c_{194}$~P in a 3:4 molar ratio ($Rv2027c_{194}$:DevR). (B) Phosphotransfer from $Rv2027c_{194}$~P to mutant DevR. $Rv2027c_{194}$~P was prepared as described. DevR-D54V, a phosphorylation-defective mutant protein, was added to $Rv2027c_{194}$~P in a 3:4 molar ratio ($Rv2027c_{194}$:DevR-D54V). The lower panel shows the Coomassie Brilliant Blue-stained gel profile of the top panel. (C) Divalent metal ion specificity in the phosphotransfer reaction to DevR from $Rv2027c_{194}$. Radiolabelled $Rv2027c_{194}$~P was prepared as described except that Ca^{2+} (at 25 mM concentration) was used in the autophosphorylation reaction instead of Mg^{2+}. After phosphorylation, $Rv2027c_{194}$ was purified free of ATP and divalent ions as described. Purified $Rv2027c_{194}$~P was then added to DevR protein (20 μM) preincubated with the specific divalent metal ion for 30 min and the reaction was allowed to proceed for 2.5 min before termination. Lane 1, Mg^{2+}; lane 2, Ca^{2+}; lane 3, Mn^{2+}; lane 4, Fe^{3+}; and lane 5, no divalent metal ion. The presence of Fe^{3+} ions in the reaction led to rapid aggregation of the proteins, which could not be resolved by SDS–PAGE.

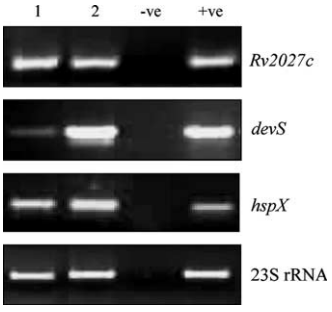

Fig. 6. RT-PCR analysis of *Rv2027c* expression in *M. tuberculosis*. Lane 1, logarithmic phase expression; lane 2, hypoxic expression; −ve, negative control containing all of the reagents except RNA; +ve, DNA positive control.

sensor kinase genes respond differentially to hypoxia; the former but not the latter is hypoxia-responsive.

A novel aspect of Rv2027c phosphorylation was the effect of Ca^{2+} that occurred via interaction with the cytoplasmic domain of Rv2027c. The vast majority of the cytoplasmic domains of histidine kinases characterized in vitro used Mg^{2+}; only TrcS from *M. tuberculosis* and EnvZ of *E. coli* utilized Ca^{2+}, the former was also noted to utilize Mn^{2+} [4,21]. Indeed as with Rv2027c, the cytoplasmic fragments of these kinases utilized Ca^{2+} as the divalent cation in autophosphorylation

reactions [4,21]. Apart from their role in in vitro autophosphorylation, Mg^{2+} and Ca^{2+} ions have also been implicated as signals sensed by two-component systems regulating virulence in *Yersinia* [22] and *Salmonella* [23]. For instance, by examining the Mg^{2+} levels in its surroundings via PhoQ protein, *Salmonella* determines its subcellular location; whereas a low (micromolar) Mg^{2+} concentration signals an intracellular environment (i.e., phagosome) a high (0.7–1 mM) Mg^{2+} concentration denotes an extracellular environment, thereby promoting entry of genes required for survival within or entry into host cells [23]. In an analogous manner, the presence of 1 mM Ca^{2+} (equivalent to the Ca^{2+} concentration in extracellular fluids) inhibited the autophosphorylation activity of Rv2027c, while micromolar and nanomolar concentrations of Ca^{2+} supported its autophosphorylation. This is well within the physiological concentration range of calcium within bacteria also, for example, 90 nM in *E. coli* [24] and of cytoplasmic calcium in resting macrophages (80–150 nM) [23], which is also a home for mycobacteria. In *M. tuberculosis*, Ca^{2+} has been established to modulate phagosome maturation in infected macrophages [25]. Distinct from the ingestion of other particles, phagocytosis of live tubercle bacilli does not induce a rise in cytosolic Ca^{2+} concentration and infection is associated with an inhibition of phagosome maturation and increased long-term survival and persistence of tubercle bacilli within macrophages [25]. The mechanism by which alterations in Ca^{2+} signalling within macrophages is coupled to mycobacterial virulence and gene expression is not known. If the in vitro autophosphorylation properties of Rv2027c over a wide range of Ca^{2+} concentrations is also extended to within the intracellular milieu, it is conceivable that activated Rv2027c could trigger an adaptation pathway through the DevR regulon within phagosomes. DevR has been recently shown to regulate the transcription of several genes during hypoxic adaptation of *M. tuberculosis* in an in vitro model of dormancy [26]. Although sequence similarities between Rv2027c and known calcium-binding proteins were not detected, the potential role of Ca^{2+} as a signalling molecule, in addition to the noted effect of Ca^{2+} on Rv2027c cytoplasmic domain function, merits further investigation.

The theme of utilization of two sensor kinases by one response regulator protein is not uncommon; sensor kinases NarQ and NarX communicate with response regulator NarL with different kinetics and modulate NarL-dependent gene expression in *E. coli* [27]. Similarly, PhoR and PhoM modulate the action of PhoB in *E. coli* [28]. These examples demonstrate that shared communication links constitute genuine functional pathways and are not mere random cross-talk events. Criss-crossing of pathways helps the organism to integrate diverse signals into a holistic response, leading to adaptation in an environment that in itself is a product of multiple signals. The common requirement for Mg^{2+} in phosphotransfer is consistent with the operation of a unified signalling pathway between the sensor kinases and DevR that would ensure regulation of a common set of genes in response to more than one signal. It is proposed that in one link of communication, DevR activity is modulated by hypoxia via phosphorelay from DevS and in a second link, DevR could be regulated through Rv2027c in response to another environmental signal. This is the first example of cross-talk between signal transduction proteins in *M. tuberculosis* and will stimulate studies of their in vivo roles in long-term survival and persistence.

Acknowledgements: Senior research fellowship from University Grants Commission to DKS and financial assistance provided to JST by the Council for Scientific and Industrial Research, Government of India is acknowledged.

References

[1] Parkinson, J.S. and Kofoid, E.C. (1992) Annu. Rev. Genet. 26, 71–112.
[2] Stock, A.M., Robinson, V.L. and Goudreau, P.N. (2000) Annu. Rev. Biochem. 69, 183–215.
[3] Himpens, S., Locht, C. and Supply, P. (2000) Microbiology 146, 3091–3098.
[4] Haydel, S.E., Dunlap, N.E. and Benjamin Jr., W.H. (1999) Microb. Pathog. 26, 195–206.
[5] Zahrt, T.C., Wozniak, C., Jones, D. and Trevett, A. (2003) Infect. Immun. 71, 6962–6970.
[6] Ewann, F., Locht, C. and Supply, P. (2004) Microbiology 150, 241–246.
[7] Saini, D.K., Malhotra, V., Dey, D., Pant, N., Das, T.K. and Tyagi, J.S. (2004) Microbiol. 150, 865–875.
[8] Cole, S.T., Brosch, R., Parkhill, J., Garnier, T., Churcher, C., Harris, D., Gordon, S.V., Eiglmeier, K., Gas, S., Barry III, C.E., Tekaia, F., Badcock, K., Basham, D., Brown, D., Chillingworth, T., Connor, R., Davies, R., Devlin, K., Feltwell, T., Gentles, S., Hamlin, N., Holroyd, S., Hornsby, T., Jagels, K., Krogh, A., McLean, J., Moule, S., Murphy, L., Oliver, K., Osborne, J., Quail, M.A., Rajandream, M.A., Rogers, J., Rutter, S., Seeger, K., Skelton, J., Squares, R., Squares, S., Sulston, J.E., Taylor, K., Whitehead, S. and Barrell, B.G. (1998) Nature 393, 537–544.
[9] Sambrook, J. and Russell, D.W. (2001) Molecular Cloning: A Laboratory Manual, third ed. Cold Spring Harbor Laboratory, Cold Spring Harbor, NY.
[10] Valdivia, R.H., Hromockyj, A.E., Monack, D., Ramakrishnan, L. and Falkow, S. (1996) Gene 29, 45–52.
[11] Saini, D.K., Pant, N., Das, T.K. and Tyagi, J.S. (2002) Protein Express Purif. 25, 203–208.
[12] Dasgupta, N., Kapur, V., Singh, K.K., Das, T.K., Sachdeva, S., Jyothisri, K. and Tyagi, J.S. (2000) Tuber. Lung Dis. 80, 141–159.
[13] Ho, Y.S., Burden, L.M. and Hurley, J.H. (2000) EMBO J. 19, 5288–5299.
[14] Freestone, P., Nyström, T., Trinei, M. and Norris, V. (1997) The Universal stress protein, UspA, of *Escherichia coli* is phosphorylated in response to stasis. J. Mol. Biol. 274, 318–324.
[15] O'Toole, R. and Williams, H.D. (2003) Res. Microbiol. 154, 387–392.
[16] Sherman, D.R., Voskuil, M., Schnappinger, D., Liao, R., Harrell, M.I. and Schoolnik, G.K. (2001) Proc. Natl. Acad. Sci. USA 98, 7534–7539.
[17] Boon, C. and Dick, T. (2002) J. Bacteriol. 184, 6760–6767.
[18] Walker, M.S. and DeMoss, J.A. (1993) J. Biol. Chem. 268, 8931–8933.
[19] Emmerich, R., Panglungtshang, K., Strehler, P., Hennecke, H. and Fischer, H.M. (1999) Eur. J. Biochem. 263, 455–463.
[20] Florczyk, M.A., McCue, L.A., Purkayastha, A., Currenti, E., Wolin, M.J. and McDonough, K.A. (2003) Infect. Immun. 71, 5332–5343.
[21] Rampersaud, A., Utsumi, R., Delgado, J., Forst, S.A. and Inouye, M. (1991) J. Biol. Chem. 266, 7633–7637.
[22] Straley, S.C., Plano, G.V., Skrzypek, E., Haddix, P.L. and Fields, K.A. (1993) Mol. Microbiol. 8, 1005–1010.
[23] Groisman, E.A. (1998) BioEssays 20, 96–101.
[24] Gangola, P. and Rosen, B.P. (1987) J. Biol. Chem. 262, 12570–12574.
[25] Malik, Z.A., Denning, G.M. and Kusner, D.J. (2000) J. Exp. Med. 191, 287–303.
[26] Park, H.D., Guinn, K.M., Harrell, M.I., Liao, R., Voskuil, M.I., Tompa, M., Schoolnik, G.K. and Sherman, D.R. (2003) Mol. Microbiol. 48, 833–843.
[27] Schröder, I., Wolin, C.D., Cavicchioli, R. and Gunsalus, R.P. (1994) J. Bacteriol. 176, 4985–4992.
[28] Amemura, M., Makino, K., Shinagawa, H. and Nakata, A. (1990) J. Bacteriol. 172, 6300–6307.